RICE CROP MONITORING USING X, C AND L BAND SAR DATA

Yuzo Suga*[1] and Tomohisa Konishi[2]
[1]Professor, Department of Global Environment Studies, Hiroshima Institute of Technology
2-1-1, Miyake, Saeki-ku, Hiroshima, 731-5193, Japan; Tel: +81-82-922-5204
Email: y.suga.mi@it-hiroshima.ac.jp

[2]Nihon CADIC Co. Ltd.,
5-33-12-102, Inokuchi, Nishi-ku, Hiroshima, 733-0842, Japan,; Tel: +81-82-270-3351;
E-mail: konishi@cadic.co.jp

KEY WORDS: Rice crop mapping, TerraSAR-X, ENVISAT-1/ASAR, ALOS/PALSAR.

ABSTRACT: Rice crop is one of the most important agricultural products in Asia. It is necessary to monitor the rice crop growth for the control and management of the cultivation. However, optical sensors have been difficulty in providing the necessary data timely for this purpose, due to cloud cover problems during the rice growing season in Asia. On the other hand, SAR has the capabilities of all-weather and night time acquisition with high resolution. This study focuses on the validation for monitoring of rice crop growth and extraction of rice-planted area using the TerraSAR-X (X-band), ENVISAT-1/ASAR (C-band) and ALOS/PALSAR (L-band) SAR data. Multi-temporal SAR data of each satellite were processed to investigate the temporal change of SAR backscattering coefficients in rice-planted area during the rice growing cycle with different wavelength, polarization and resolution in Hiroshima, Japan. Ground truth data were measured simultaneously with satellite observation such as height of plant, vegetation cover rate and leaf area index. The correlation coefficients between backscattering coefficients and plant height in HH and HV of TerraSAR-X SptLight mode were 0.9864 and 0.9196, respectively. The correlation coefficients between one and vegetation cover in HH and HV of TerraSAR-X were 0.9921 and 0.9549, respectively. The correlation coefficients between one and LAI in HH and HV of TerraSAR-X were 0.9953 and 0.9971, respectively. In addition, we attempt to produce a rice crop map using three kinds of temporal SAR data sets consisted of TerraSAR-X, ENVISAT-1/ASAR and ALOS/PALSAR. The rice-planted area is extracted from the multi-temporal SAR data based on a classification using maximum likelihood method. The precision ratio of the rice crop map using TerraSAR-X, ASAR and PALSAR was 77.3 %, 48.5 % and 57.7 %, respectively. As the result, rice crop growth and rice-planted area extraction can be successfully performed using multi-temporal and multi-wavelength SAR data.

1. INTRODUCTION

Rice is the most important agricultural product in Asia region, and numerous workforces are still necessary to produce and to monitor the rice crop every year. Optical remotely sensed images have been expected to monitor the rice crop growth; however, these images have been difficulty in providing the necessary data timely, due to cloud cover problems during the rice planting season in Japan. Space-borne synthetic aperture radar (SAR) has all-weather and night time acquisition capabilities with high resolution. SAR data have a potential of rice crop monitoring at regular intervals.

In past years, some papers concerning the rice crop monitoring with SAR data were reported. Rice crop growth monitoring using L-band SAR (JERS-1/SAR) had some difficulties in providing adequate monitoring because the temporal change of L-band SAR backscatter was influenced by the alignment of rice crop fields and the rice planting orientation (Rosenqvist, 1999). C-band radar image, the backscatter intensity of ERS-1,2/SAR (VV) and RADARSAT (HH) images change remarkably from non-cultivated bare soil conditions before rice crop is planted due to the irrigated conditions just after rice planting (Suga et al., 1999). According to this characteristic, rice-planted area extraction can be performed by means of the change of SAR backscattering. In generally, there are two major methods for producing a rice map. One is a method of identification by using threshold of SAR data before and after rice planting. The other is a method of classification by using multi-temporal SAR data (Kurosu et al., 1997). A rice map produced by SAR data is useful in terms of early estimation of rice field area and distribution.

In Japan, a lot of farmland are comparatively small, and also locate in mountainous region. In recent year, space-borne SAR satellite of high resolution has been launched such as the German TerraSAR-X satellite which has a capability of rice crop monitoring in each small rice fields according to high resolution performance.

In this study, the authors investigate rice crop growth monitoring by using X, C and L-band SAR data. The objective

is to understand the behavior of each SAR backscatter from rice crop field and to verify the correlation between SAR backscatter and ground truth measurements in small rice field in Japan. In addition, we attempt to produce a rice map by using multi-temporal SAR data and to verify the rice map in comparison with the one produced by aerial photograph.

2. TEST SITE AND TEST DATA

2.1 Test site

The test site is Aki-Takata City in Hiroshima Prefecture in the western part of Japan. This site has typical paddy fields around Hiroshima Prefecture in which the rice planting period is almost same. The rice planted area of Aki-Takata City was 2,450 ha in the total of 27,060 ha of Hiroshima Prefecture in 2007 (The Ministry of Agriculture, Forestry and Fisheries of Japan, 2007).

2.2 Ground truth data

The ground truth measurements are performed simultaneously with SAR observation. In each ground truth data, physical parameters such as plant height, vegetation cover and leaf area index (LAI) relevant to rice growth conditions are measured and also ground photographs are taken in the rice crop field using a digital camera. The height of crop is calculated by the average of 12 points in the test field. The vegetation cover is calculated from binary image which is classified into two categories such as rice plant and soil in rice field. LAI is based on optical assumption concerning amount of leaf and attenuation of light using plant canopy analyzer (LI-COR LAI-2000).

As for the condition of paddy field, rice crop field is filled with water from May to the beginning of June after planting, blade of rice crop grows up in July. Rice ear bears fruit at the beginning of August, and then the rice crop is harvested from the end of August to September.

2.3 SAR data used in this study

TerraSAR-X is a high resolution X-band SAR satellite launched in 2007. TerraSAR-X has a spatial resolution of 1m in SpotLight mode with 10km swath and 3m in StripMap mode with 30km swath. This SAR is much better than conventional SAR in terms of the spatial resolution. ENVISAT-1/ASAR is a C-band SAR launched in 2002. ASAR has a spatial resolution of 30m in alternating polarization (AP) mode with 100km swath. ALOS/PALSAR is a L-band SAR launched in 2006. PALSAR has a spatial resolution of 10m with 70km swath in high resolution mode. The system parameters of SAR data used in this study are listed in Table 1. TerraSAR-X data were taken on 2008, and ASAR and PALSAR data were taken in the same season on 2007.

Table 1. The specification of SAR used in this study.

Satellite	TerraSAR-X		ENVISAT-1/ASAR	ALOS/PALSAR
Mode	SpotLight	StripMap	Alternating Polarization	High Resolution
Frequency	9.65GHz (X)		5.331GHz (C)	1.27GHz (L)
Polarization	HH	HH/HV	HH/VV	HH
Incidence angle (deg.)	32.5	29.4	28.7	34.3
Nominal resolution(m)	1	3	30	10
Swath (km)	10	30	100	70
Acquisition date	26-Apr-2008	19-Apr-2008	2-May-2007	21-Apr-2007
	20-Jun-2008	30-Apr-2008	19-May-2007	06-Jun-2007
	23-Jul-2008	11-May-2008	6-Jun-2007	22-Jul-2007
		22-May-2008	23-Jun-2007	
		2-Jun-2008	11-Jul-2007	
		24-Jun-2008	28-Jul-2007	
		5-Jul-2008		
		27-Jul-2008		

2.4 SAR data processing

SAR data have to convert from digital number to backscattering coefficients for rice crop monitoring. ENVISAT-1/ASAR data are directly down linked by the ground station of Hiroshima Institute of Technology (HIT). TerraSAR-X data have already processed by the DLR at level 1b product. The radar backscattering coefficient (σ^0) of TerraSAR-X is estimated as shown in Eq. (1) (Fritz et al., 2007)

$$\sigma^0 = 10 \log_{10}(calFactor * DN^2 * \sin\alpha) \ [\text{dB}] \quad (1)$$

where *DN* is digital number of an amplitude image pixel, *calFactor* is calibration constant, α is incidence angle at the target pixel.

ASAR data are processed by VEXCEL SAR Processor (APEX 2002) to make Precision Image (PRI) product, two look amplitude data (16-bit) with 12.5m pixel size. The σ^0 of ASAR is estimated as shown in Eq. (2) (Rosich et al., 2004)

$$\sigma^0 = 10 \log_{10}(DN^2 / K * \sin\alpha) \ [\text{dB}] \quad (2)$$

where *DN* is digital number of an amplitude image pixel, *K* is absolute calibration constant, α is incidence angle at the target pixel.

PALSAR data are processed by Japan Aerospace Exploration Agency (JAXA) at level 1.5. The σ^0 of PALSAR is estimated as shown in Eq. (3) (JAXA, 2008)

$$\sigma^0 = 10 \log_{10}(DN^2) + CF \ [\text{dB}] \quad (3)$$

where *DN* is digital number of an amplitude image pixel, CF is constant factor.

In this experiment, the average backscattering coefficients are used over rice-planted area to reduce the influence of speckle noise.

3. DATA ANALYSIS

3.1 Temporal backscatter behavior in rice field

The backscattering coefficients of SAR were depicted from TerraSAR-X (X-band), ASAR (C-band) and PALSAR (L-band) in the test site where is consisted of two rice fields (Rice-A and Rice-B, each size is 85m x 43m). The numbers of pixels used for the measurement are 255 for TerraSAR-X StripMap mode, 2184 for TerraSAR-X SpotLight mode, 25 for ASAR and 72 for PALSAR, respectively. Figure 1 shows the temporal change in SAR backscattering coefficients with TerraSAR-X StripMap mode. σ^0_{HH} of Rice-A and Rice-B in 13 days before transplanting are considerably different because Rice-A is covered with rough soil surface, on the other hand, Rice-B is covered with water before transplanting. Around transplanting period, the surface of rice fields are covered with water, then σ^0_{HH} shows around -40 dB and σ^0_{HV} shows around -43 dB. Rice seedling development seasons from 20 to 50 days after transplanting, then σ^0_{HH} increases to -10 dB and σ^0_{HV} increases to -33 dB. At the phase from 55 to 90 days, σ^0_{HH} decreases to -18 dB and σ^0_{HV} decreases to -35 dB. Figure 2 shows the temporal change in SAR backscattering coefficients with TerraSAR-X SpotLight mode. σ^0_{HH} shows around -35 to -40 dB on water surface in both rice fields before transplanting. σ^0_{HH} of SpotLight mode increase to around -13 dB at 49 days after transplanting. Then, σ^0_{HH} of SpotLight mode decrease around -16 dB. These temporal change patterns are similar to σ^0_{HH} of TerraSAR-X StripMap mode. Figure 3 shows the temporal change in SAR backscattering coefficients with ASAR. σ^0_{HH} of ASAR shows around -11 dB and σ^0_{VV} shows around -7 dB in 17 days after transplanting. These values of ASAR are higher than those of TerraSAR-X. Then, σ^0_{HH} increase from -11 to -2 dB and σ^0_{VV} increase from -11 to -5 dB. σ^0_{HH} of C-band SAR is higher than σ^0_{VV} during rice crop growth. Figure 4 shows the temporal change in SAR backscattering coefficients with PALSAR. σ^0_{HH} of PALSAR shows around -17 dB in 35 days after transplanting. Then, σ^0_{HH} of PALSAR shows around -13 dB in 81 days after transplanting. These values are almost equal to σ^0_{HH} of PALSAR before transplanting. The range of σ^0_{HH} of PALSAR is approximately 4 dB. The range of σ^0 shows the smallest value of HH polarization in comparison with TerraSAR-X and ENVISAT-1/ASAR.

X-band SAR backscattering coefficients in rice fields of the test site change remarkably in these three SAR bands. The change of X-band backscattering coefficients of HH polarization is approximately 30 dB. This change appears until 50 days after transplanting. Then, the backscattering coefficients decrease in comparison with other SAR data. C-band SAR shows that the backscattering coefficients with HH polarization indicate the highest value at -2 dB. In addition, the backscattering coefficients of HH polarization increase linearly until 90 days after transplanting. It may be useful to monitor the rice growing cycle. L-band SAR shows that the range of the backscattering coefficients in rice fields is the smallest in comparison with HH polarization of X and C-band SAR.

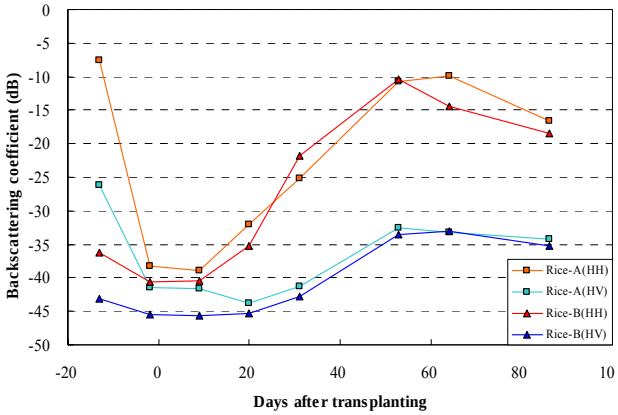

Fig. 1. Temporal change in SAR backscattering coefficients with TerraSAR-X StripMap mode in 2008.

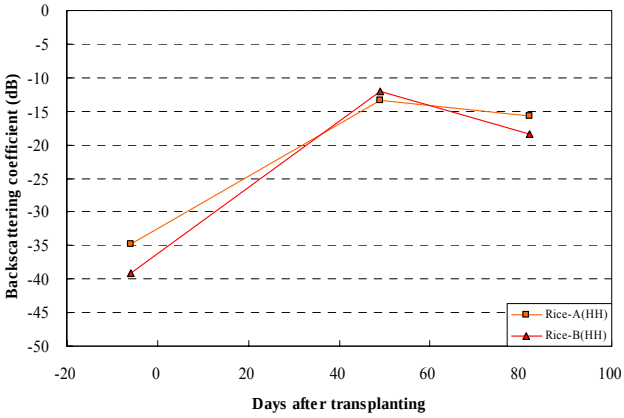

Fig. 2. Temporal change in SAR backscattering coefficients with TerraSAR-X SpotLight mode in 2008.

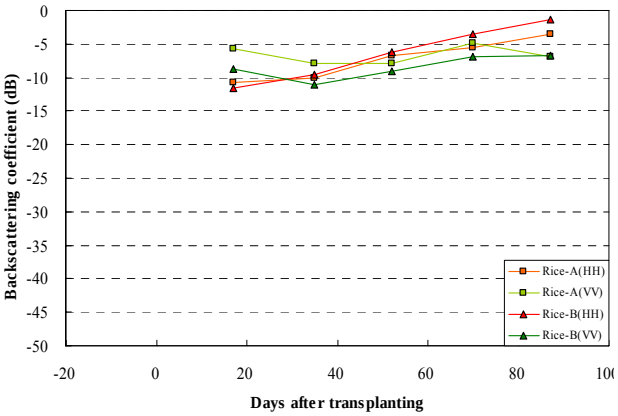

Fig. 3. Temporal change in SAR backscattering coefficients with ENVISAT-1/ASAR AP mode in 2007.

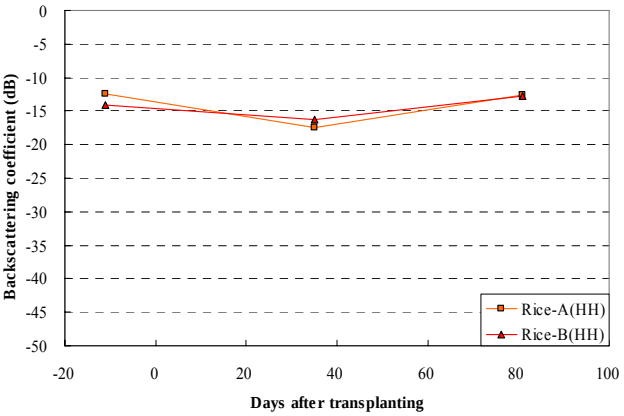

Fig. 4. Temporal change in SAR backscattering coefficients with ALOS/PALSAR High Resolution mode in 2007.

3.2 Comparison between ground truth data and SAR backscatter in rice fields

In order to derive physical parameters from SAR backscatter in rice fields, a regression analysis is performed. Ground truth measurements are simultaneously performed with TerraSAR-X observation in 2008. The parameters of measurements are plant height, vegetation cover and leaf area index (LAI) in rice fields of the test site. The correlation coefficients in HH and HV between backscattering coefficients and plant height are 0.9864 and 0.9196, respectively. The correlation coefficients in HH and HV between backscattering coefficients and vegetation cover are 0.9921 and 0.9549, respectively. The correlation coefficients in HH and HV between backscattering coefficients and LAI are 0.9953 and 0.9971, respectively. All correlation coefficients are very high, and also vegetation cover is linearly correlated with backscattering coefficients in HV polarization. The results show the possibility that vegetation cover can be derived from TerraSAR-X HV polarization data.

3.3 Rice crop mapping

A rice crop mapping is useful to monitor on the rice crop production management. There is a possibility to produce the rice crop map using SAR data during the rice crop growth. In addition, high resolution SAR data is more useful to discriminate land cover information such as road, house, river, farmland and forest around rice fields.

In previous study (Suga et al., 1999), the combination of three kinds of cases which are before rice planting, just after rice planting and early phase of growing by using RADARSAT data could extract rice planted area in early phase of rice growing season by means of maximum likelihood classifier (MLC). In this study, we attempt to produce a rice crop map using three kinds of temporal SAR data sets consisted of TerraSAR-X, ENVISAT-1/ASAR and

ALOS/PALSAR. TerraSAR-X data are acquired on 30 April, 2 June and 5 July in 2008. ASAR data are acquired on 2 May, 6 June and 11 July in 2007. PALSAR data are acquired on 21 April, 6 June and 2 July in 2007 as shown in Table 1.

At first, speckle suppression filtering is processed in order to reduce a speckle noise on SAR images. Median filter is applied in a manner of 5 x 5 moving window. The second step, all SAR images are overlaid onto the topographic map with 1:25,000 scale. Then, the foreshortening of SAR images are corrected by using digital elevation model (DEM) with 50 meters spatial resolution. The datasets are merged as three temporal SAR images including two polarization modes of TerraSAR-X and ASAR, respectively and single polarization mode of PALSAR.Finally, rice crop maps are produced by the above temporal SAR images by means of maximum likelihood classifier. Prior to produce a rice map, the existing rice crop fields are digitized on a topographic map and an aerial photograph taken on 2003 for the validation of rice crop mapping. On the other hand, house, river, forest, and rice fields are selected as categories of land cover in the temporal SAR images. Training area data for supervised classification are selected in reference to topographic map and ground truth. Then, each binary image related with rice field and other category is produced as shown in Figure 5 to 8. As these images are still contaminated by speckle noise, the majority filter with a 7 x 7 window is applied to reduce it.

The validation method of the rice crop map adopts the true production rate (TPR) and the false production rate (FPR). TPR is the coincidence rate of rice-planted areas derived from temporal SAR images within those derived from aerial photograph, on the other hand, FPR is the rate of non-rice-planted areas derived from aerial photograph within rice-planted areas derived from temporal SAR images.

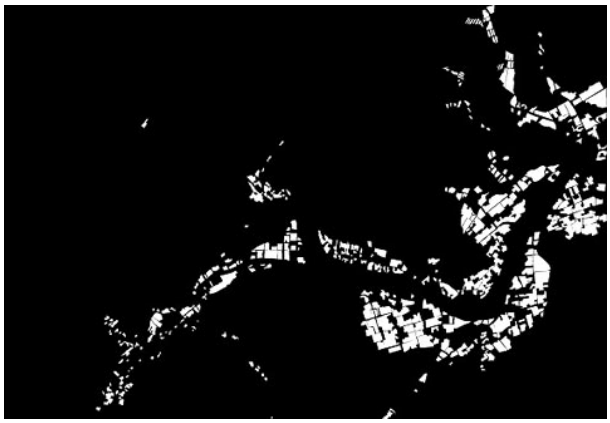

Fig. 5. Rice crop maps by Aerial photograph.

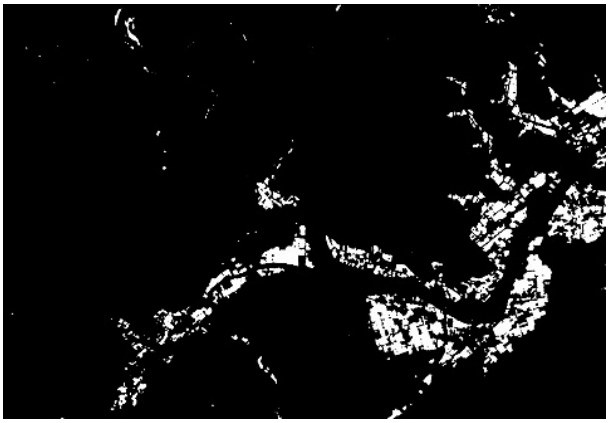

Fig. 6. Rice crop maps by TerraSAR-X

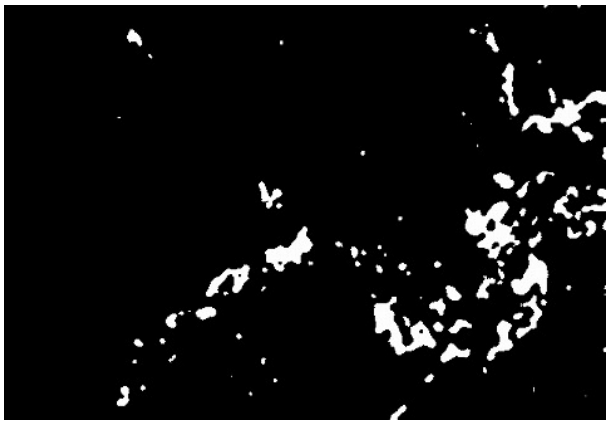

Fig. 7. Rice crop maps by ENVISAT-1/ASAR.

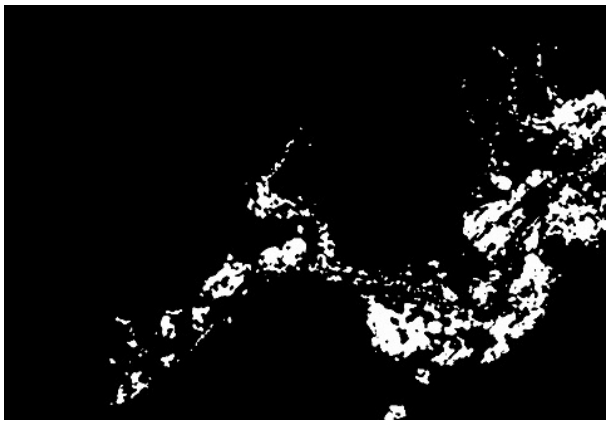

Fig. 8. Rice crop maps by ALOS/PALSAR.

(White color shows rice-planted area)

Table 2 shows the results of rice crop map validation in comparison with the rice crop areas derived from topographic map and aerial photograph. TPR and FPR calculated from TerraSAR-X are 77.3 % and 26.8 %, respectively. This result shows that TerraSAR-X with X-band high resolution has an advantage in terms of spatial resolution for the extraction of rice planted area.

On the other hand, ASAR and PALSAR have lower values of TPR than one of TerraSAR-X. The spatial resolution of ASAR is lower than TerraSAR-X and PALSAR. ASAR with C-band contains strong backscatter area in rice field

around houses because the multiple reflection effect spreads strong return signal to surrounding pixels. Therefore, 30 m spatial resolution is insufficient for rice-planted area extraction because strong backscatter cannot be distinguished from backscatter of rice fields in the test site. PALSAR with L-band is difficult to extract a rice field precisely because the temporal change is smaller than TerraSAR-X and ASAR in early phase of rice growing cycle. However, TPR of PALSAR is better than one of ASAR. There is a reason why the spatial resolution of PALSAR is better than that of ASAR. FPR of PALSAR is the worst in three kinds of temporal SAR data sets because dry riverbed areas are classified into rice fields. The backscatter in dry riverbed area is similar to rice field in the test site. TPRs except TerraSAR-X are relatively low in this experiment because a rice field is relatively small and located near residences in the test site. In addition, the test site is located in mountainous area, then the registration error still remains in mountainous areas due to the residual of foreshortening correction in this experiment.

Table 2. The results of rice crop map validation.

Satellite	TPR (True production rate) (%)	FPR (False production rate) (%)
TerraSAR-X StripMap	77.3	26.8
ENVISAT-1/ASAR	48.5	30.6
ALOS/PALSAR	57.7	49.7

4 CONCLUSIONS

Rice crop growth monitoring was attempted by using multi-temporal X, C and L-band SAR data. We have two objectives in which one is to understand SAR backscatter behavior in rice field of different acquisition band SAR data, and the other is to verify rice crop map produced by multi-temporal SAR data. The backscattering coefficients of TerraSAR-X StripMap mode data change from -40 to -10 in HH polarization and from -45 to -32 dB in HV polarization. And also, TerraSAR-X is useful resources as the best of three kinds of temporal SAR data sets for rice crop monitoring using backscattering coefficients of temporal change until 90 days after transplanting.ENVISAT-1 /ASAR shows that the backscattering coefficients with HH polarization indicate the highest value at -2 dB in these SAR data. In addition, the backscattering coefficients in HH polarization increase linearly until 90 days after transplanting. It is useful to monitor on the rice growing cycle. ALOS/PALSAR shows that the range of the backscattering coefficients in rice field is the smallest compared with X and C-band SAR with HH polarization.

Finally, rice crop mapping was attempted using multi-temporal SAR data taken on an early phase of rice growing season. The overall rice crop distribution patterns extracted from these SAR data sets showed relatively good coincidence with the rice crop area derived from aerial photograph in the small test site. Especially, TerraSAR-X showed fairly good coincidence with the one which is typical rural agriculture area in Japan.

Acknowledgments

This study was conducted as a part of Strategic Research Infra-structure Construction Project in Hiroshima Institute of Technology, entitled on “Generation of time-spatial image information using earth observation satellite remote sensing”, supported by the Ministry of Education, Culture, Sports, Science and Technology, Japan.

TerraSAR-X data used in this study were provided through TerraSAR-X Science Service System based on the contract with DLR.

References

Fritz, T., Mittermayer, J., Schattler, B., Balzer, W., Buckreub, S. and Werninghaus, R., 2007. TerraSAR-X Ground Segment Level 1b Product Format Specification, DLR.

JAXA, 2008. ALOS PALSAR Level 1 Product Format Description, Vol.2, Rev.K.

Kurosu, T., Fujita, M. and Chiba, K., 1997. The identification of rice fields using multi-temporal ERS-1 C band SAR data, International Journal of Remote Sensing 18(14), pp. 2953-2965.

Rosenqvist, A., 1999. Temporal and spatial characteristics of irrigated rice in JERS-1 L-band SAR data, International Journal of Remote Sensing 20(8), pp. 1567-1587.

Rosich, B. and Meadows, P., 2004. Absolute calibration of ASAR Level 1 products generated with PF-ASAR, ESRIN.

Suga, Y., Oguro, Y., Takeuchi, S. and Tsuchiya, K., 1999. Comparison of various SAR data for vegetation analysis over Hiroshima city, Advances in Space Research 23(8), pp. 1509-1516.

The Ministry of Agriculture, Forestry and Fisheries of Japan, 2007. Statistics on Crops, <http://www.maff.go.jp/j/tokei/>.